

PAPER • OPEN ACCESS

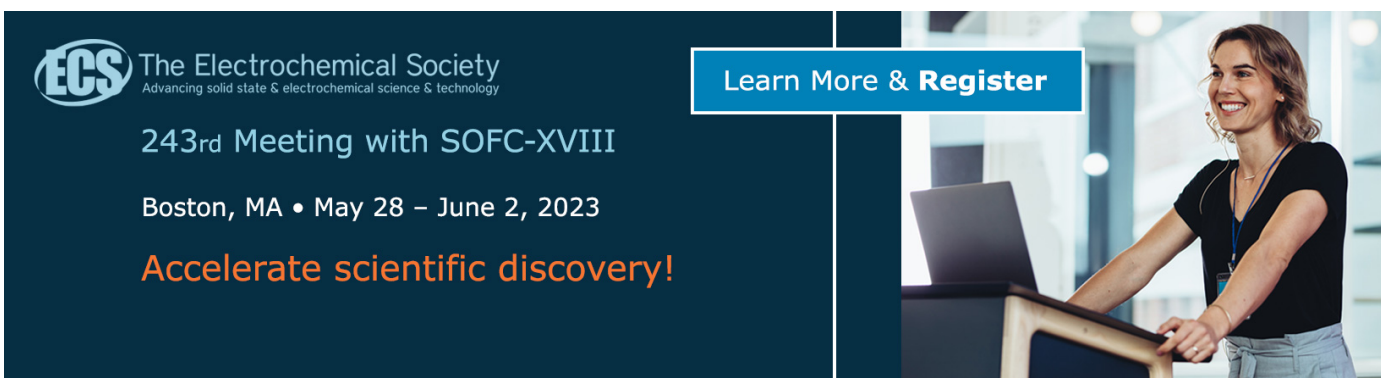
## Study of the GERDA Phase II background spectrum

To cite this article: M. Agostini *et al* 2017 *J. Phys.: Conf. Ser.* **888** 012106

View the [article online](#) for updates and enhancements.

### You may also like

- [A new calibration method for charm jet identification validated with proton-proton collision events at  \$s = 13\$  TeV](#)  
The CMS collaboration, Armen Tumasyan, Wolfgang Adam et al.
- [Search for Multimessenger Sources of Gravitational Waves and High-energy Neutrinos with Advanced LIGO during Its First Observing Run, ANTARES, and IceCube](#)  
A. Albert, M. André, M. Anghinolfi et al.
- [Identification of hadronic tau lepton decays using a deep neural network](#)  
A. Tumasyan, W. Adam, J.W. Andrejkovic et al.



**ECS** The Electrochemical Society  
Advancing solid state & electrochemical science & technology

243rd Meeting with SOFC-XVIII

Boston, MA • May 28 – June 2, 2023

**Accelerate scientific discovery!**

Learn More & Register

# Study of the GERDA Phase II background spectrum

M. Agostini<sup>a</sup>, M. Allardt<sup>d</sup>, A.M. Bakalyarov<sup>m</sup>, M. Balata<sup>a</sup>, I. Barabanov<sup>k</sup>, L. Baudis<sup>s</sup>, C. Bauer<sup>g</sup>, E. Bellotti<sup>h,i</sup>, S. Belogurov<sup>l,k</sup>, S.T. Belyaev<sup>m</sup>, G. Benato<sup>s</sup>, A. Bettini<sup>p,q</sup>, L. Bezrukov<sup>k</sup>, T. Bode<sup>o</sup>, D. Borowicz<sup>c,e</sup>, V. Brudanin<sup>e</sup>, R. Brugnera<sup>p,q</sup>, A. Caldwell<sup>n</sup>, C. Cattadori<sup>i</sup>, A. Chernogorov<sup>l</sup>, V. D'Andrea<sup>a,\*</sup>, E.V. Demidova<sup>l</sup>, N. Di Marco<sup>a</sup>, A. Domula<sup>d</sup>, E. Doroshkevich<sup>k</sup>, V. Egorov<sup>e</sup>, R. Falkenstein<sup>r</sup>, N. Frodyma<sup>c</sup>, A. Gangapshev<sup>k,g</sup>, A. Garfagnini<sup>p,q</sup>, C. Gooch<sup>n</sup>, P. Grabmayr<sup>r</sup>, V. Gurentsov<sup>k</sup>, K. Gusev<sup>e,m,o</sup>, J. Hakenmüller<sup>g</sup>, A. Hegai<sup>r</sup>, M. Heisel<sup>g</sup>, S. Hemmer<sup>q</sup>, W. Hofmann<sup>g</sup>, M. Hult<sup>f</sup>, L.V. Inzhechik<sup>k</sup>, J. Janicskó Csáthy<sup>o</sup>, J. Jochum<sup>r</sup>, M. Junker<sup>a</sup>, V. Kazalov<sup>k</sup>, T. Kihm<sup>g</sup>, I.V. Kirpichnikov<sup>l</sup>, A. Kirsch<sup>g</sup>, A. Kish<sup>s</sup>, A. Klimenko<sup>g,e</sup>, R. Kneißl<sup>n</sup>, K.T. Knöpfle<sup>g</sup>, O. Kochetov<sup>e</sup>, V.N. Kornoukhov<sup>l,k</sup>, V.V. Kuzminov<sup>k</sup>, M. Laubenstein<sup>a</sup>, A. Lazzaro<sup>o</sup>, V.I. Lebedev<sup>m</sup>, B. Lehnert<sup>d</sup>, H.Y. Liao<sup>n</sup>, M. Lindner<sup>g</sup>, I. Lippi<sup>q</sup>, A. Lubashevskiy<sup>g,e</sup>, B. Lubsandorzhev<sup>k</sup>, G. Lutter<sup>f</sup>, C. Macolino<sup>a</sup>, B. Majorovits<sup>n</sup>, W. Maneschg<sup>g</sup>, E. Medinaceli<sup>p,q</sup>, M. Miloradovic<sup>s</sup>, R. Mingazheva<sup>s</sup>, M. Misiaszek<sup>c</sup>, P. Moseev<sup>k</sup>, I. Nemchenok<sup>e</sup>, D. Palioselitis<sup>n</sup>, K. Panas<sup>c</sup>, L. Pandola<sup>b</sup>, K. Pelczar<sup>c</sup>, A. Pullia<sup>j</sup>, S. Riboldi<sup>j</sup>, N. Rumyantseva<sup>e</sup>, C. Sada<sup>p,q</sup>, F. Salamida<sup>i</sup>, M. Salathe<sup>g</sup>, C. Schmitt<sup>r</sup>, B. Schneider<sup>d</sup>, S. Schönert<sup>o</sup>, J. Schreiner<sup>g</sup>, O. Schulz<sup>n</sup>, A.-K. Schütz<sup>r</sup>, B. Schwingenheuer<sup>g</sup>, O. Selivanenko<sup>k</sup>, E. Shevzik<sup>e</sup>, M. Shirchenko<sup>e</sup>, H. Simgen<sup>g</sup>, A. Smolnikov<sup>g,e</sup>, L. Stanco<sup>q</sup>, L. Vanhoefer<sup>n</sup>, A.A. Vasenko<sup>l</sup>, A. Veresnikova<sup>k</sup>, K. von Sturm<sup>p,q</sup>, V. Wagner<sup>g</sup>, A. Wegmann<sup>g</sup>, T. Wester<sup>d</sup>, C. Wiesinger<sup>o</sup>, M. Wojcik<sup>c</sup>, E. Yanovich<sup>k</sup>, I. Zhitnikov<sup>e</sup>, S.V. Zhukov<sup>m</sup>, D. Zinatulina<sup>e</sup>, K. Zuber<sup>d</sup>, G. Zuzel<sup>c</sup>.

<sup>a</sup>) LNGS & GSSI (INFN), <sup>b</sup>) LNS (INFN), <sup>c</sup>) IoP Cracow, <sup>d</sup>) TU Dresden, <sup>e</sup>) JINR Dubna, <sup>f</sup>) EU, Geel, <sup>g</sup>) MPI Heidelberg, <sup>h</sup>) U. Bicocca Milan, <sup>i</sup>) INFN Bicocca Milan, <sup>j</sup>) U.d.Studi Milan, <sup>k</sup>) INR Moscow, <sup>l</sup>) ITEP Moscow, <sup>m</sup>) Kurchatov Moscow, <sup>n</sup>) MPI Munich, <sup>o</sup>) TUM Munich, <sup>p</sup>) U. Padova, <sup>q</sup>) INFN Padova, <sup>r</sup>) EKUT Tübingen, <sup>s</sup>) U. Zurich <sup>\*</sup>) presenter

E-mail: gerda-eb@mpi-hd.mpg.de

**Abstract.** The GERDA experiment, located at the Laboratori Nazionali del Gran Sasso (LNGS) of INFN in Italy, searches for the neutrinoless double beta ( $0\nu\beta\beta$ ) decay of  $^{76}\text{Ge}$ . GERDA Phase II is aiming to reach a sensitivity for the  $0\nu\beta\beta$  half life of  $10^{26}$  yr in  $\sim 3$  years of physics data taking with 100 kg·yr of exposure and a background index of  $\sim 10^{-3}$  cts/(keV·kg·yr). After 6 months of acquisition a first data release with 10.8 kg·yr of exposure is performed, showing that the design background is achieved. In this work a study of the Phase II background spectrum, the main spectral structures and the background sources will be presented and discussed.

## 1. GERmanium Detector Array

The GERDA setup is designed to minimize the main background sources which affected the previous generation experiments. High-purity germanium detectors are mounted in low mass ultra-pure holders and are directly inserted in liquid argon (LAr). The most part of detectors is made from material with  $^{76}\text{Ge}$  isotope fraction enlarged to about 86%. The argon cryostat is complemented by a water tank with 10 m diameter which further shields from neutron and  $\gamma$  backgrounds. A description of the experimental setup is given in Ref. [1].

A first physics data taking campaign (Phase I) was carried out from November 2011 to June



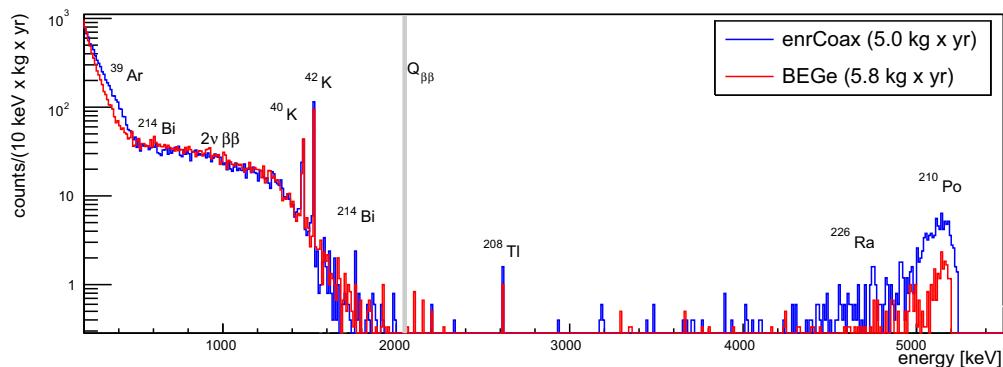


**Figure 1.** Normalized GERDA Phase II spectra, before pulse shape discrimination and LAr veto, for BEGe (red) and  $^{enr}\text{Ge}$  coaxial (blue) detectors. The prominent features and the  $Q_{\beta\beta}$  region (where the  $0\nu\beta\beta$  decay is expected) are indicated

2013 and the results [2] showed no indication of a  $0\nu\beta\beta$  signal. After the completion of Phase I the GERDA setup has been upgraded to perform its next step (Phase II): the goal was the tenfold reduction of the background, optimizing the experimental setup, and the increase of the  $^{enr}\text{Ge}$  detector mass. Thirty Broad Energy Germanium (BEGe) detectors from Canberra [3] were deployed: they allow superior background rejection and have an excellent energy resolution. In addition an active suppression of background by detecting the LAr scintillation light, consisting of PMTs and wavelength shifting fibers coupled to silicon photomultipliers, has been introduced.

On December 20th, 2015 the Phase II data taking with all 40 detectors (30 BEGes, 7  $^{enr}\text{Ge}$  and 3  $^{nat}\text{Ge}$  coaxial detectors) started. The first Phase II data were released after 6 months, corresponding to an exposure of 10.8 kg·yr of  $^{enr}\text{Ge}$  (5.0 kg·yr from  $^{enr}\text{Ge}$  coaxial detectors and 5.8 kg·yr from BEGes).

## 2. GERDA Phase II background spectrum

Fig. 1 shows the background spectra of Phase II after quality cuts, and before applying the pulse shape discrimination and the LAr veto. The spectra for the 2 types of detectors (BEGes in red and  $^{enr}\text{Ge}$  coaxial detectors in blue) are normalized by their current exposure.

The spectra show the expected prominent structures: the low energy region up to 500 keV is dominated by the long-lived  $^{39}\text{Ar}$  isotope ( $\beta$ -emitter with  $T_{1/2} = 269$  yr and  $Q = 565$  keV); from 600 to 1400 keV the  $2\nu\beta\beta$  spectrum shows up; next the 1461 keV and 1525 keV  $\gamma$ -lines from  $^{40}\text{K}$  and  $^{42}\text{K}$  respectively are visible;  $\gamma$ -lines from  $^{238}\text{U}$  and  $^{232}\text{Th}$  chains are also visible and the high energy region ( $> 3500$  keV) shows the  $\alpha$ -structures from  $^{210}\text{Po}$  ( $Q = 5.41$  MeV) and  $^{226}\text{Ra}$  ( $Q = 4.87$  MeV).

From the pulse shape of the observed  $\alpha$  events, it can be determined that they are mostly located at the  $p^+$  contact surface. There is a large variation of the rate among the detectors (Fig. 2) and the origin of the contamination is not understood.

The time dependence of the  $\alpha$  rate in  $^{enr}\text{Ge}$  coaxial detectors shows an exponential decay with  $T_{1/2} = 177 \pm 36$  days (Fig. 3), a value compatible with  $^{210}\text{Po}$  ( $T_{1/2} = 138$  days) and a minor contribution from  $^{226}\text{Ra}$  chain (constant).

The intensities of the visible or expected  $\gamma$ -lines has been estimated with a Bayesian fit, the results are shown in Table 1 together with the Phase I values from Ref. [4].

The count rate of  $^{40}\text{K}$  is higher with respect to Phase I by a factor of  $\sim 4$ . This could be explained by the increased number of cables and detector holders and by the introduction of the LAr instrumentation. The rate of the  $^{42}\text{K}$   $\gamma$ -line is about twice compared to Phase I where

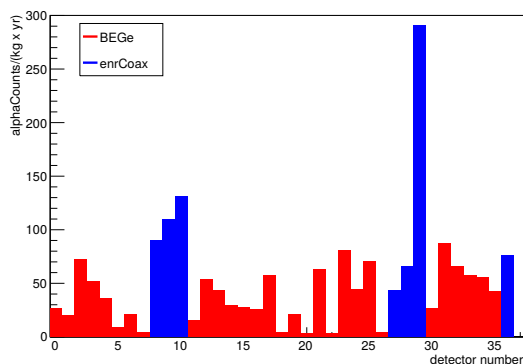


**Figure 2.**  $\alpha$  count rate per detector normalized to exposure

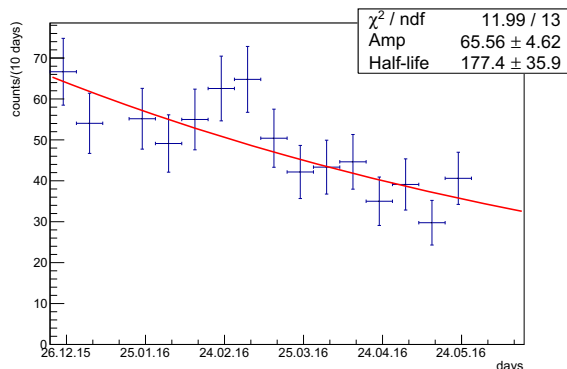


**Figure 3.**  $\alpha$  count rate versus time for  $^{enr}\text{Ge}$  coaxial detectors

**Table 1.** Normalized count rate of indicated  $\gamma$ -lines: mode and smallest 68% interval or 90% limit

	energy [keV]	Phase II		Phase I	
		BEGe rate [cts/(kg-yr)]	$^{enr}\text{Coax}$ rate [cts/(kg-yr)]	BEGe rate [cts/(kg-yr)]	$^{enr}\text{Coax}$ rate [cts/(kg-yr)]
$^{40}\text{K}$	1460.8	$50.3^{+2.5}_{-3.4}$	$55.4^{+3.3}_{-3.9}$	$12.7^{+3.2}_{-3.1}$	$14.1^{+1.1}_{-1.2}$
$^{42}\text{K}$	1524.7	$88.0^{+4.8}_{-3.0}$	$113.0^{+4.3}_{-5.6}$	$46.6^{+4.6}_{-4.9}$	$60.6^{+2.0}_{-1.8}$
$^{214}\text{Bi}$	609.3	$8.9^{+2.8}_{-2.3}$	$8.0^{+3.5}_{-2.8}$	$12.0^{+6.2}_{-5.3}$	$8.1^{+2.2}_{-2.5}$
	1120.3	$2.6^{+1.2}_{-1.8}$	$3.6^{+2.3}_{-2.0}$	$6.7^{+4.0}_{-4.2}$	$< 2.9$
	1764.5	$0.8^{+0.5}_{-0.4}$	$2.0^{+0.8}_{-0.6}$	$< 2.5$	$3.2 \pm 0.5$
$^{208}\text{Tl}$	583.2	$7.6^{+3.5}_{-2.8}$	$< 5.3$	$< 11.0$	$4.0^{+2.2}_{-2.1}$
	2614.5	$1.0^{+0.5}_{-0.4}$	$1.7^{+0.7}_{-0.6}$	$0.6^{+0.7}_{-0.5}$	$1.5 \pm 0.4$
$e^+ \text{ ann}$	511	$12.6^{+3.4}_{-3.4}$	$11.9^{+3.7}_{-3.1}$	$16.5^{+6.4}_{-6.1}$	$10.4^{+2.4}_{-2.6}$

metallic shrouds shielded the LAr volume from the electric fields surrounding the detectors and HV cables. Phase II needs transparent non-metallic shrouds to readout the LAr scintillation light, allowing electric field to be dispersed in LAr hence to move  $^{42}\text{K}$  ions. This affects the top detectors more than the others.

From the  $^{238}\text{U}$  chain the most intense  $^{214}\text{Bi}$   $\gamma$ -lines are observed with rates on the same level of Phase I and the ratios between lines of different energy indicate that the  $^{214}\text{Bi}$  sources are located not only within the Ge array but also outside.  $^{208}\text{Tl}$   $\gamma$ -lines (from  $^{232}\text{Th}$  chain) are also visible, the intensities are small as in Phase I and don't allow to indicate the source position at such level of statistics. The 511 keV  $\gamma$ -line (“ $e^+$  ann” in Table 1) is observed in the spectra too.

### 3. Conclusions

The study of the GERDA Phase II background spectrum showed the presence of  $\gamma$  and  $\alpha$  structures also visible in the Phase I spectrum. The composition of the observed background and the localization of the various sources are information needed to build the background model and to understand which contributions are expected in the region around the  $Q_{\beta\beta}$  value.

**Acknowledgement:** The Gerda experiment is supported financially by BMBF, DFG, INFN, MPG, NCN, RFBR, and SNF. The institutions acknowledge also internal financial support.

### References

- [1] GERDA Collaboration, Eur. Phys. J. C (2013) **73** 2330
- [2] GERDA Collaboration, Phys. Rev. Lett. **111**, 122503 (2013)
- [3] D. Budjás et al., J. Instrum. **4**, P10007 (2009)
- [4] GERDA Collaboration, Eur. Phys. J. C (2014) **74** 2764